Elastodynamic modeling and inversion with reflectivity terms

Cosmin Macesanu, Guanghui Huang, Faqi Liu, Jaime Ramos-Martinez and Dan Whitmore, TGS*

Summary

Significant advancements have recently been achieved in the use of full waveform inversion (FWI) methods for the derivation of high-resolution model parameters. In comparison to implementations using the acoustic approximation, it has been shown that accounting for elastic effects through the use of elastic equations significantly enhances the quality of inversion results. Additional improvements can be achieved by employing variable density parametrizations; however, the low frequency component of the density model is notoriously challenging to constrain properly. An alternative approach is aiming for the reconstruction of high frequency components of the density model, which can be achieved by reparametrizing the elastic equations in term of impedance or reflectivity. We demonstrate the benefits of this new parameterization by comparing synthetic data obtained from elastic impedance inversion to field data from an OBN survey.

Introduction

The additional physics embedded in the elastic wave equation enables elastic FWI (EFWI) to outperform the acoustic version in geologically complex areas like those with strong velocity contrast or areas associated with a reservoir showing abnormal AVO effects (Liu et al., 2024). However, in such areas (as well as for AVO) varying density effects may be as important as shear-wave effects. In the context of acoustic inversion, there are many examples showing the benefit of accounting for variable density through the inversion of impedance or reflectivity models (Yang et al., 2021; Rayment et at., 2023; Burren et al., 2025). This is achieved by a reparameterization of the acoustic equations in terms of velocity and impedance or reflectivity (Whitmore et al. 2020). We extend this approach to the elastic case, by reparametrizing the elastic equation in terms of impedance. We discuss the new formulation and demonstrate its accuracy and utility from synthetic and field data examples.

Theory

We start from the standard formulation of the elastic equations in terms of the stress and velocity variables:

$$\frac{\partial \tau_{ij}}{\partial t} = c_{ijkl}\frac{\partial v_k}{\partial x_l} + I_{ij}(x) \qquad (1a)$$

$$\frac{\partial v_i}{\partial t} = \frac{1}{\rho}\frac{\partial \tau_{ij}}{\partial x_j} \quad . \qquad (1b)$$

The elements of the stiffness tensor c_{ijkl} are evaluated in terms of physical parameters such as the P and S wave velocities V_p, V_s, the density ρ, and Thomsen (1986) parameters for anisotropic media. Following the approach in Macesanu et al. (2024), we can redefine the stiffness components and velocity variables by scaling with the input density model:

$$v_i = \frac{v_i^0}{\rho}\,, \qquad c_{ijkl} = c^0{}_{ijkl}\,\rho \qquad (2)$$

This leads to the following equations:

$$\frac{\partial \tau_{ij}}{\partial t} = c^0{}_{ijkl}\frac{\partial v_k^0}{\partial x_l} - c^0{}_{ijkl}\frac{\partial \ln \rho}{\partial x_l} v_k^0 + I_{ij}(x) \qquad (3a)$$

$$\frac{\partial v_i^0}{\partial t} = \frac{\partial \tau_{ij}}{\partial x_j} \quad . \qquad (3b)$$

In this formulation, the effect of variable density is encapsulated in the reflectivity terms proportional to $\partial \ln \rho$. This explains why there is little sensitivity to the low frequency components of the density field.

It is furthermore desirable to replace density as a parameter by the logarithm of the acoustic impedance $\ln I_p = \ln(\rho V_p)$. This is advantageous both in terms of reducing cross-talk between parameters (Operto et al., 2013), and additionally by relating the parametrization of the elastic equations to measurable medium properties (impedance) useful for quantitative interpretation. Using the impedance as a free parameter also allows the separation of the FWI gradient in a low frequency component used for updating the background velocity and a high frequency component contributing to model reflectivity (Douma et al., 2010; Ramos-Martinez et al., 2016).

After reparameterization, the stress update equation (3a) becomes:

$$\frac{\partial \tau_{ij}}{\partial t} = c^0{}_{ijkl}\frac{\partial v_k^0}{\partial x_l} - c^0{}_{ijkl}\frac{\partial \ln\left(\frac{I_p}{V_p}\right)}{\partial x_l} v_k^0 + I_{ij}(x) \quad . \qquad (4)$$

Reflectivity components can be obtained either by taking the derivative of the logarithmic impedance after inversion, or by treating the reflectivity components as free parameters in the inversion (Whitmore et al. 2020). These fields may be defined by

$$2\, r_i = \frac{\partial \ln I_p}{\partial x_i} = \frac{1}{\rho}\frac{\partial \rho}{\partial x_i} + \frac{1}{V_p}\frac{\partial V_p}{\partial x_i}\,. \qquad (5)$$

We note that since these fields are not independent, for an inversion problem parametrized in terms of reflectivity the objective function should include additional constraints.

Examples

To illustrate the effects of the new equations with new parametrization (replacing density with impedance) we generate synthetic data using Eqs. (1) and (4) for the SEAM elastic model. Figure 1a) shows the logarithmic impedance in the area used for data simulation. Figures 2a) and 2b) show respectively synthetic data generated with input density (Eqs. 1), and data generated with input log-impedance (Eq. 4). The differences in the two results are minimal and can be explained by numerical differences in the implementation of the finite difference solution for the elastic equations.

We note however that in practice one is not able to derive an impedance model similar to that of Fig 1a) from the inversion of field data. Typically, impedance models derived by inversion lack some of the low frequency components; to test the effect of the missing components, we remove the low frequency in the original model by applying a radial (Laplacian) filter in space domain. The resulting filtered log-impedance is shown in Fig 1b); data generated using this model is displayed in Fig 2c). By comparison with the data generated with full bandwidth impedance we see that the synthetics are substantially similar, thus indicating that inverting for a bandpassed-version of logarithmic impedance model can lead to a successful match with the input/field data.

One of the benefits of using impedance/reflectivity as an independent parameter in inversions is that it allows for a better match with the field data. To illustrate this, we show an example from an inversion of an OBN dataset from Brazil. We apply a workflow consisting of a velocity-only phase matching inversion scheme (Elastic Dynamic Matching FWI), followed by multiparameter inversion employing scale separation for the velocity and impedance gradients, as described in Huang et al. (2024). Figures 3a) and 3b) show the velocity model (inline and crossline sections). The velocity model provides good kinematic

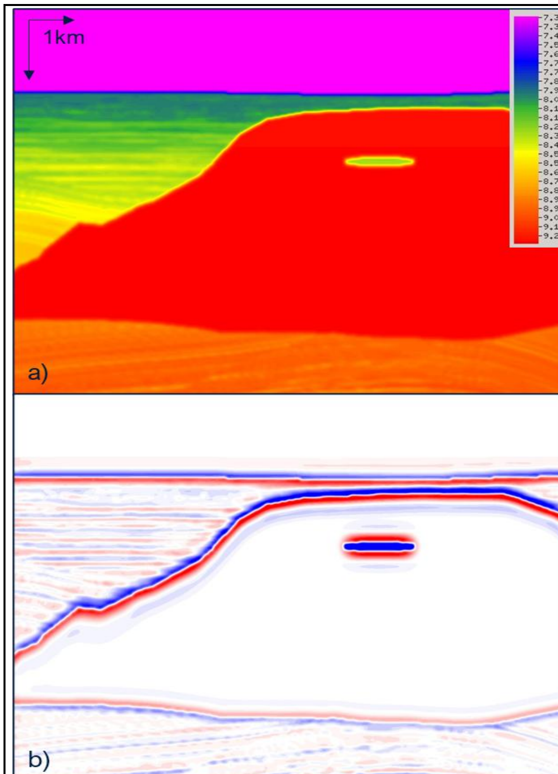

Figure 1: Models used for generating synthetic data: a) logarithmic impedance b) filtered log-impedance

match for the events in the data, however, since the E-

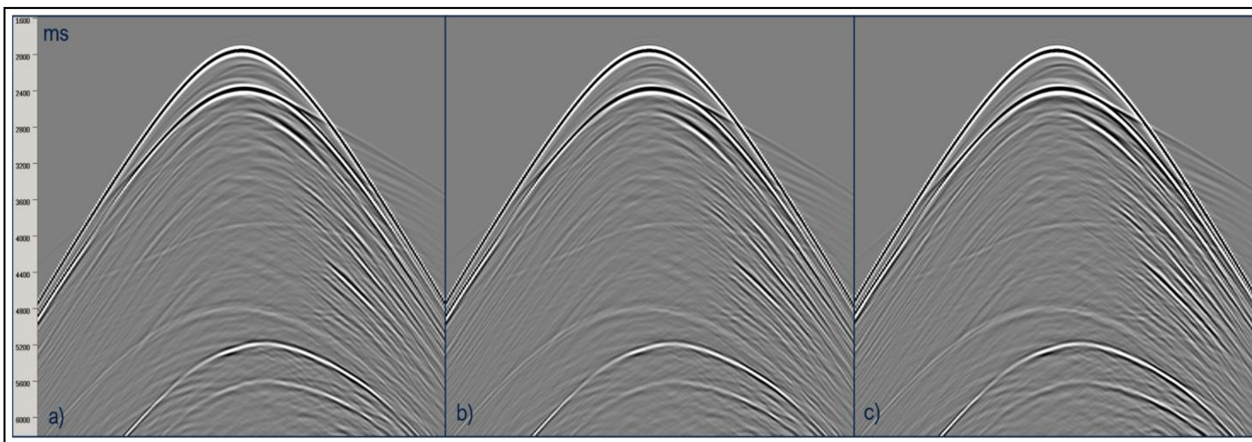

Figure 2: Synthetic data generated with: a) density model b) log-impedance model and c) filtered log-impedance.

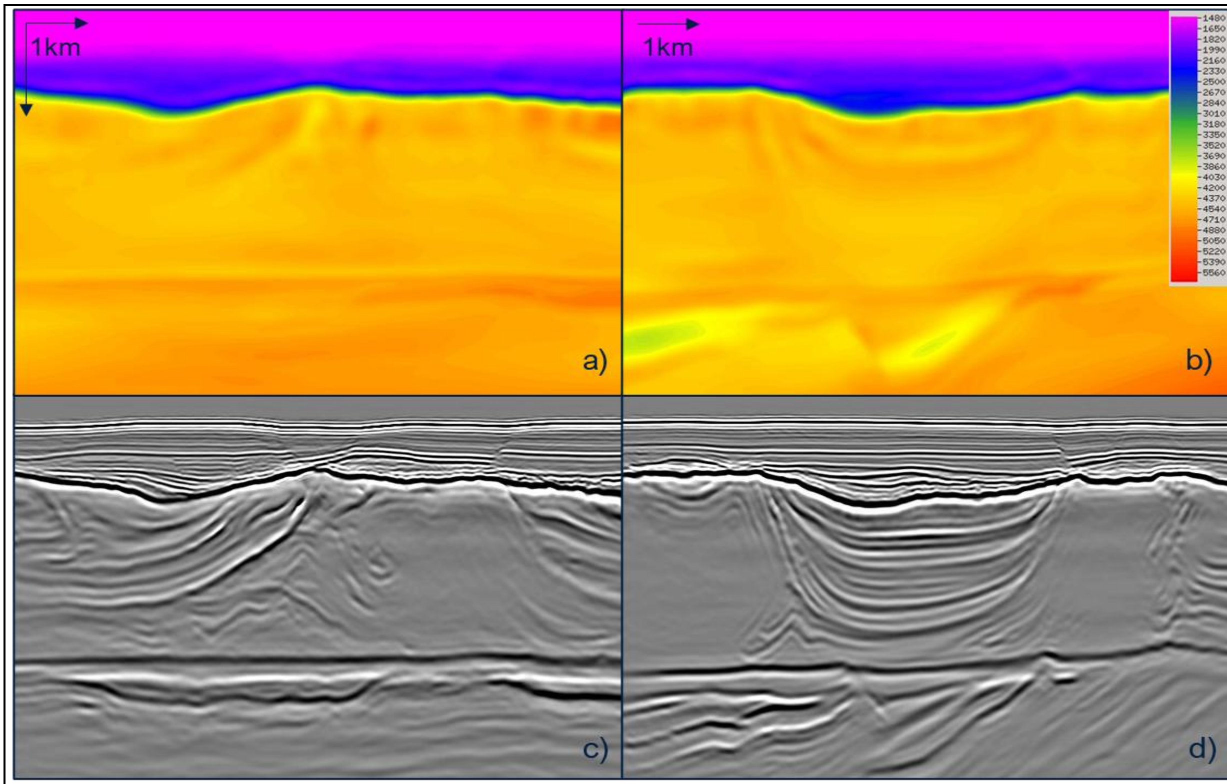

Figure 3: Inversion results from OBN field data, showing velocity model (top) and normal reflectivity (bottom); left : inline section, right : crossline section.

DMFWI cost function emphasizes the phase of the events, amplitude information is suppressed, and as a result the high frequency components of the model are attenuated. The multiparameter inversion stage which employs an L2 cost function sensitive to amplitude generates these higher frequency components and inserts them mostly into the impedance parameter. Figures 3c) and 3d) show the normal reflectivity, derived from the derivatives of the impedance and local dip structure. As expected, the normal reflectivity model shows significantly higher frequency content compared to velocity.

For data comparison, Figure 4a) shows a common receiver gather from the OBN dataset. The top of the salt primary event and reflections off the salt base and pre-salt strata are indicated by arrows. Later events are multiples. Figure 4b) shows the synthetic gather after the application of the multiparameter inversion workflow for velocity and impedance update. One can note a good match between the input data and the synthetic, in terms of phase as well as amplitude, for both primaries and multiples. This indicates a successful inversion for both velocity and acoustic impedance.

Conclusions

The success of full waveform inversion relies on the accuracy of the equations used to model the field data. Increasing the complexity of the physics embedded in the modeling equations bring the synthetic simulation closer to the ground truth. Thus, moving from the acoustic approximation to elastic equations brings significant benefits in the quality of inversion results. Accounting for the effects of varying density constitutes a further improvement in the accuracy of seismic modeling and inversion.

In this abstract we have presented a form of the elastic equations where the effects of variable density are parametrized in terms of an acoustic impedance model, a quantity easier to estimate from surface seismic data. We have shown that this parametrization produces equivalent results to the standard equations. Moreover, we have shown

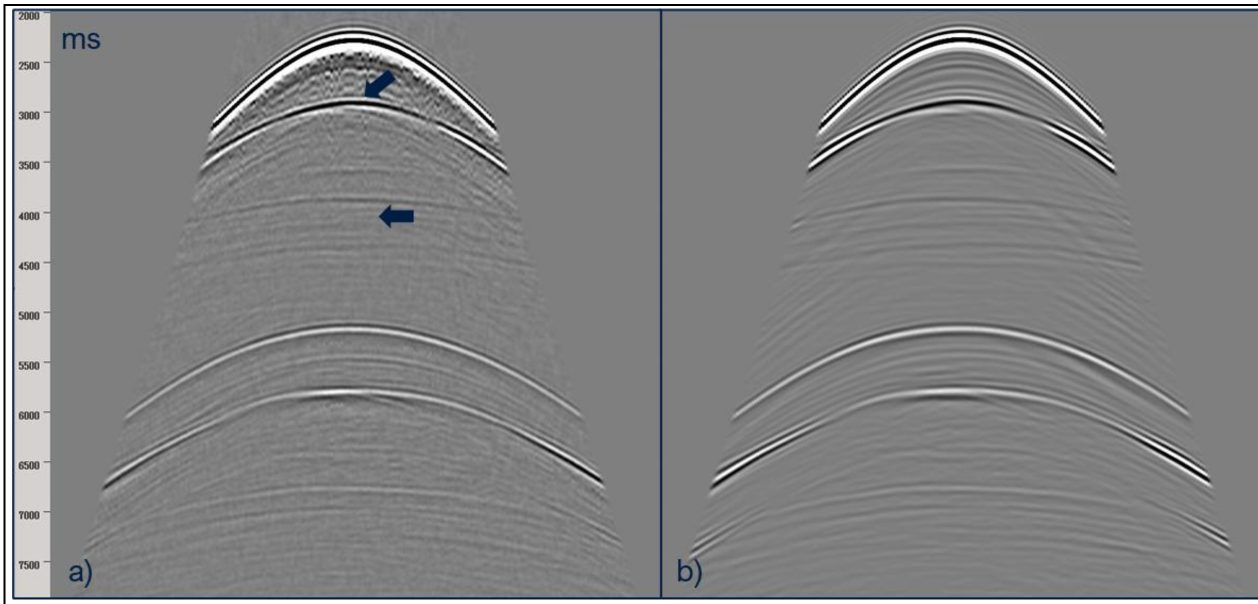

Figure 4: a) OBN receiver gather field data b) synthetic gather following velocity + impedance inversion

that taking into account impedance through a multiparameter approach (which inverts for impedance in addition to velocity) improves the match of the synthetic to field data, which is expected to benefit the inversion process.

Acknowledgements

We thank TGS for permission to publish these results, and Petrobras for providing the field dataset.